Effects of Intratumoral Competition on Allowable Treatment Breaks under Immune-Mediated Tumor Control

Wimonnat Sukpol[1], Teeraphan Laomettachit[2], and Anuwat Tangthanawatsakul[1,*]

[1]Department of Mathematics, Faculty of Science, King Mongkut's University of Technology Thonburi, Bangkok, Thailand
[2]Bioinformatics and Systems Biology Program, School of Bioresources and Technology, King Mongkut's University of Technology Thonburi, Bangkok, Thailand

Abstract. In this study, we investigated the effects of intratumoral competition and intermittent immunotherapy on tumor population dynamics using numerical simulations. We focused on how the immune-mediated elimination rate of the dominant tumor subtype, together with the duration of treatment withdrawal jointly determine treatment outcomes. Our results demonstrate that achieving an optimal balance between reducing the population of stronger cancer cells and preventing the regrowth of weaker cancer cells is essential for effective tumor suppression. Both the immune-mediated elimination efficiency and the length of treatment withdrawal critically determine the maximum allowable treatment break that maintains the total tumor burden below a control threshold. We further show that higher competition ratios significantly shrink the optimal regions for immune response. These findings provide quantitative insights into the design of intermittent treatment strategies that enhance innate immune effectiveness while maintaining tumor control.

1 Introduction

Tumor heterogeneity is widely recognized as a fundamental challenge in cancer treatment. Intratumor heterogeneity refers to the concept of heterogeneity within one particular tumor. These divergent cellular properties often lead to divergent functionality, causing intricate dynamics within the carcinoma cells [1]. Tumor heterogeneity has been observed in different types of cancers, such as leukemia, breast, prostate, colon, brain, esophagus, head and neck, bladder, gynecological carcinomas, liposarcoma, and multiple myeloma [2]. However, an important consideration is that having phenotypic diversity within a tumor means that drug treatments targeting one population may not affect another population. Consequently, the tumor may shrink but could contain resistant or weaker forms that could survive and ultimately reemerge. This could lead to drug treatment failure and recurrence [3]. Heterogeneous tumors also have another characteristic in the form of cancer stem cells (CSCs). Cancer stem cells have properties that include self-renewal and the ability to initiate the re-growth of the tumor, even after a substantial reduction in the tumor [4]. Immunotherapy, a new innovative technique in cancer treatment, relies on the human immune system to combat cancer. Recent advances in immunotherapy have significantly improved patient outcomes and survival rates when compared to current treatments like radiation, chemotherapy, and surgery [5].

In previous work [6], we examined how enhanced immune activity can be exploited in the presence of asymmetric intratumoral competition, where one tumor subtype possesses a competitive advantage over the others. In particular, we modeled preferential immune targeting of the dominant tumor subtype by increasing its immune-mediated elimination rate. From a clinical perspective, this modelling framework captures therapeutic strategies aimed at boosting innate immune activity, for example through the activation of natural killer cells or related innate immune mechanisms [7]. These strategies were shown to effectively suppress the dominant tumor population under continuous treatment assumptions.

Nevertheless, continuous enhancement of immune activity is often clinically infeasible due to risks such as immune exhaustion, cumulative toxicity, and adverse effects. Therefore, treatment interruptions or withdrawal periods are unavoidable in practice. Motivated by these considerations, the present study extends previous modeling frameworks by incorporating intermittent immunotherapy into a heterogeneous tumor system. We focus on the interplay between intratumoral competition and immune-mediated targeting of the dominant tumor subtype under withdrawal schedules. In particular, we examine how immune elimination rate and withdrawal duration jointly influence tumor population dynamics through numerical simulations.

2 Mathematical model

In this study, the mathematical model is adopted from [6]. This model considers two populations of cancer stem cell denote by C_1 and C_2, two populations of the

* Corresponding author: anuwat.sae@kmutt.ac.th

corresponding tumor cells (x_1, x_2) and the innate immune cell I. The following five ordinary differential equations govern the system dynamics :

$$\frac{dC_1}{dt} = r_1 C_1\left(1-\frac{C_1}{M_1}\right) - \beta_1 C_1 I \quad (1)$$

$$\frac{dC_2}{dt} = r_2 C_2\left(1-\frac{C_2}{M_2}\right) - \beta_2 C_2 I \quad (2)$$

$$\frac{dx_1}{dt} = k_1 C_1\left(\frac{C_1}{M_1}\right)\left(1-\frac{x_1}{M_3}\right) - n_1 x_1 - \beta_3 x_1 I - b_{12} x_1 x_2 \quad (3)$$

$$\frac{dx_2}{dt} = k_2 C_2\left(\frac{C_2}{M_2}\right)\left(1-\frac{x_2}{M_4}\right) - n_2 x_2 - \beta_4 x_2 I - b_{21} x_1 x_2 \quad (4)$$

$$\frac{dI}{dt} = s - n_3 I \quad (5)$$

This formulation captures logistic growth CSCs, tumor cell production driven by CSC, immune suppression, and competition between tumor subpopulations. The immune component represents innate immune cells (natural killer cells), modeled with a constant recruitment rate and a natural death rate. All variables and parameters retain the same biological interpretation as in [6] and are summarized in Table 1. In this work, this model serves as a reference framework for the numerical simulations presented in the following sections, where the effects of immune modulation under intratumoral competition are investigated.

3 Numerical simulation

All numerical simulations were performed using MATLAB (version 9.7). The simulations are conducted based on the mathematical model described in the previous section, with parameter values listed in Table 1. Following the biological assumptions commonly adopted in competitive tumor models [8], we consider a heterogeneous tumor composed of two cancer subtypes with asymmetric competitive abilities. In particular, x_2 is assumed to be the more aggressive population, characterized by a stronger competitive effect on subtype 1 $(b_{12} > b_{21})$. In the first scenario, the ratio of b_{12} / b_{21} is 2. Motivated by this competitive asymmetry, the immune response is assumed to primarily target the stronger subtype and is modeled by increasing the immune-mediated elimination rates of cancer stem cells and tumor cells associated with subtype 2, represented by β_2 and β_4, during treatment periods, reflecting enhanced innate immune cytotoxicity [7]. When treatment is withdrawn, these parameters are returned to their baseline values. In the present work, we investigate how variations in β_2 interact with treatment interruption, with particular emphasis on the maximum allowable treatment break duration that still maintains tumor control.

3.1. The effect of β_2 and break periods

Previous study in [6] have indicated that the immune-mediated elimination rate β_2 plays a crucial role in controlling the dominant tumor subtype. The simulation in Fig. 1a held the immunotherapy duration fixed at 5 days, and varied the withdrawal duration and the value of β_2. This approach has been analyzed to cover actual scenarios in which patients may not tolerate high-dose treatments and lengthier withdrawal times must be considered. The outcomes are color-coded. Green represents cases where $C_1 + C_2 + x_1 + x_2 < 10^6$, indicating effective tumor control. Yellow corresponds to cases where $C_1 + C_2 + x_1 + x_2 \geq 10^6$, but both $C_1 + x_1$ and $C_2 + x_2$ remain below the threshold of 10^6. Yellow is divided into two shades: light yellow represents cases where $C_2 + x_2 < C_1 + x_1$, while dark yellow corresponds to scenarios where $C_1 + x_1 < C_2 + x_2$. Light orange represents scenarios where $C_1 + x_1 \geq 10^6$ while $C_2 + x_2 < 10^6$.

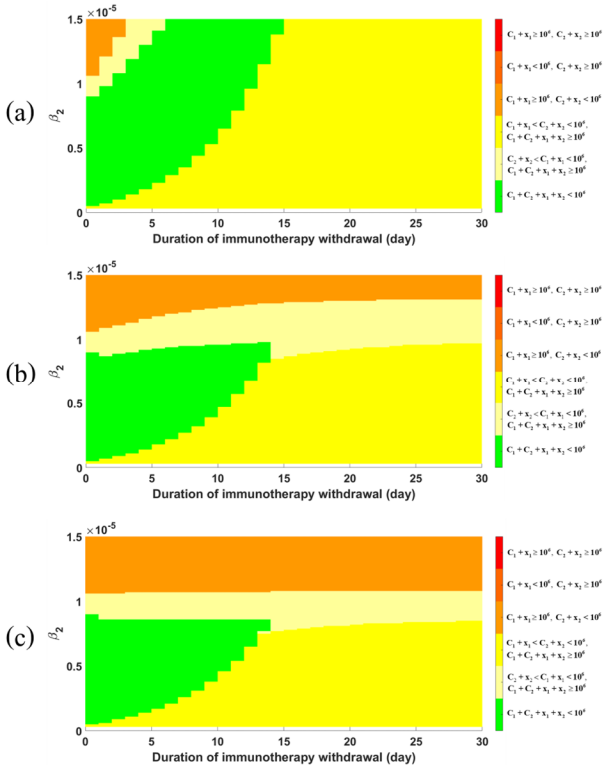

Fig. 1. Total number of cancerous cell population under varying immunotherapy withdrawal durations and β_2 with fixed $\beta_4 = 4\times10^{-6}$ for different treatment duration. (a) 5 days. (b) 15 days. (c) 30 days.

To provide a better understanding of the dynamics for each color area in Fig. 1a, we simulate to examine the dynamics of cells in each population. The value of β_2 was fixed at 1.3×10^{-5} and withdrawal durations were varied as follows: 1 day (light orange), 3 days (light yellow), 8 days (green), and 16 days (dark yellow). Fig. 2a shows the light orange region, where $C_2 + x_2$ (black

Table 1. Parameters used in all numerical simulations.

Parameter	Unit	Value	Interpretation	Ref
r_1, r_2	day^{-1}	0.75	Division rate of C_1, C_2	[1]
k_1, k_2	day^{-1}	0.514	Division rate of x_1, x_2	[9]
M_1, M_2	cells	$1.5\% \times M_{\text{total}}$	Carrying capacity of C_1, C_2	[10]
M_3, M_4	cells	10^7 to 10^9	Carrying capacity of x_1, x_2	[11], [12]
n_1, n_2	day^{-1}	0.01	Natural death rate of x_1, x_2	[13]
β_1, β_2	$\text{cell}_I^{-1}\text{day}^{-1}$	3×10^{-7}	Death rate of C_1, C_2 due to I response	[1]
β_3, β_4	$\text{cell}_I^{-1}\text{day}^{-1}$	3×10^{-6}	Death rate of x_1, x_2 due to immune response	[1]
s	cell/day	1.3×10^4	Source rate of I	[9]
n_3	day^{-1}	0.29	Natural death rate of I	[9]
b_{12}	$\text{cell}_{x_2}^{-1}\text{day}^{-1}$	4.87×10^{-6} to 5×10^{-5}	The competition effect of x_2 on x_1	Vary
b_{21}	$\text{cell}_{x_1}^{-1}\text{day}^{-1}$	2.92×10^{-6} to 10^{-5}	The competition effect of x_1 on x_2	Vary

line) decreases rapidly, allowing $C_1 + x_1$ (red line) to rise beyond 10^6. During withdrawal period, $C_1 + x_1$ decreases slightly, while $C_2 + x_2$ increases but not enough to suppress $C_1 + x_1$, resulting in $C_1 + x_1 \geq 10^6$.

Fig. 2b represents the light-yellow region. A high dose of β_2 rapidly eliminates the strong cancerous type, allowing the sensitive cancerous type to rebound and drive the total population above 10^6. Additionally, the too-short withdrawal duration prevents $C_2 + x_2$ from recovering sufficiently to suppress $C_1 + x_1$, leading to a persistently high cancerous population.

Fig. 2c represents the green (optimal) region. During treatment, the $C_2 + x_2$ decrease but remains viable. After an 8-day drug withdrawal, $C_2 + x_2$ regrows sufficiently to suppress $C_1 + x_1$, keeping total population below 10^6.

Fig. 2d show dark yellow region. While $C_2 + x_2$ declines during treatment, a 20-day drug withdrawal allows it to grow significantly. Although $C_2 + x_2$ remains below 10^6, the combined total of $C_1 + C_2 + x_1 + x_2$ slightly exceeds 10^6.

Next, simulations were conducted by varying the treatment duration to 15 and 30 days, as shown in Fig. 1b and 1c. As the treatment duration increases from 5 to 15 and 30 days (Fig. 1), green region area shrinks, suggesting that less optimal combinations between β_2. and the duration of drug withdrawal are available. On the other hand, the light yellow and light orange areas expand, indicating a higher likelihood that the total cancerous population will exceed 10^6 due to the rebound of the weak cancer type. This suggests that eliminating strong cancer cells too aggressively allows the weak type to overgrow. These results suggest that therapy with shorter cycles interrupted by breaks may be more effective at keeping the cancer growth below the threshold.

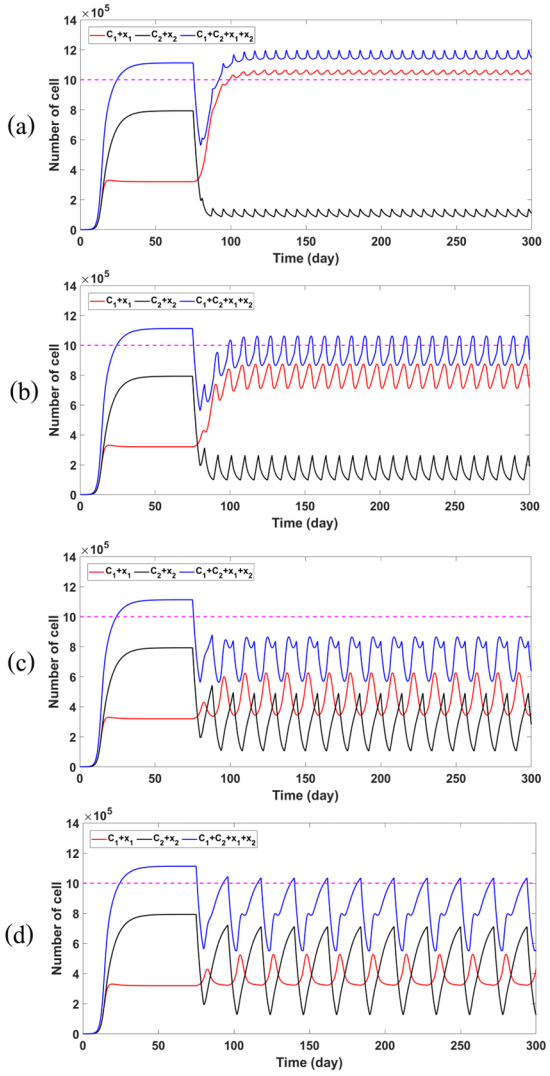

Fig. 2. Population dynamics of cells under different immunotherapy withdrawal schedules with fixed $\beta_2 = 1.3\times10^{-5}, \beta_4 = 4\times10^{-6}$ (a) 1 day break period (light orange region) (b) 3 day break period (light yellow region) (c) 8 day break period (green region) (d) 16 day break period (dark yellow region).

3.2. The effects of intratumoral competition and break periods on cancer population dynamics

The competition ratio between populations x_1 and x_2 can vary and potentially affecting both the immunotherapy withdrawal period and the optimal value of β_2 . In this section, we explore how different competition ratios, b_{12} to b_{21}, influence tumor dynamics. The simulations fix the treatment duration at 5 days, while varying the competition ratio between b_{12} and b_{21} into three cases.

With a competition ratio of 2 (Fig. 3a), the green area is largest in all three cases and appears with a balance between the value of β_2 and the duration of immunotherapy withdrawal. In Fig. 3b and Fig. 3c, the green area decreases significantly, indicating a reduced range of conditions where the total tumor population remains below 10^6. Interestingly, the right side of the figure shows a transition from the yellow region to a dark orange region, where it marks cases where $C_1 + x_1 < 10^6$, but $C_2 + x_2 \geq 10^6$. This occurs due to the increased competition (both at 5 and 16 times), which enables the strong population to outcompete the weak population more effectively. When the drug withdrawal period is too long, the strong population can rebound, even if a relatively high treatment dose is applied. This recovery enables it to suppress the weak population, leading to an overall increase in tumor burden.

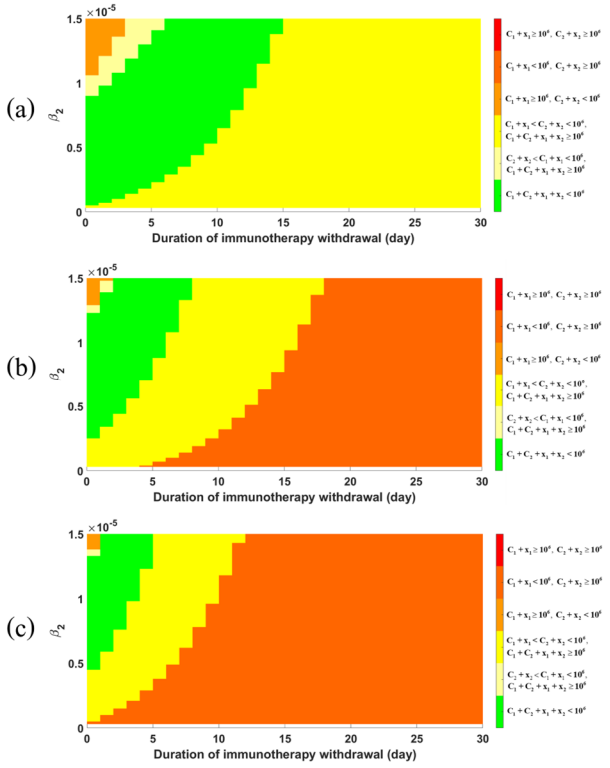

Fig. 3. Simulated total number of cancerous cells with different durations of immunotherapy withdrawal and value of β_2 with fixed treatment duration 5 days. (a) competition ratio is two times. (b) competition ratio is five times. (c) competition ratio is sixteen times.

This result highlights the complex interplay between intratumoral competition, drug dosage, and withdrawal duration. The balance between suppressing the strong population and maintaining the weak population is critical. Overkilling the strong type with short treatment breaks may create conditions where the weak population expands, leading to a total cancer cell count exceeding 10^6 (light orange or light-yellow regions). On the other hand, insufficient suppression combined with prolonged treatment breaks may allow the strong population to recover, also resulting in a total cell count exceeding 10^6 (dark yellow or dark orange regions). Thus, balancing the treatment dose and the duration of treatment breaks (green area) allows both types to coexist, leading to better overall control.

3.3. The effects of large treatment dosages and durations on cancer population dynamics

To explore the effects of high intratumoral competition, increased β_4 , and prolonged treatment, we conduct additional simulations with competition ratios of 2, 5, and 16 while setting β_4 to a high value 10^{-4} and extending the treatment duration to 30 days. This setup allows us to determine whether stronger competition, combined with prolonged treatment and high β_4 , results in a new red region, where both the strong and weak populations exceed the threshold ($C_1 + x_1$ and $C_2 + x_2$ both exceed 10^6), leading to uncontrolled tumor growth.

It can be observed from Fig. 4 that when intratumoral competition increases, red areas emerge when a large dose β_2 is administered for a prolonged period of time. The red areas indicate the strong and weak populations are above 10^6, denoting uncontrolled tumor growth. The red areas primarily appear at the upper-right corners of the plots, i.e., for extended treatment withdrawal and large values of β_2 . In Fig. 4a with a competition ratio of 2, there are no red areas. However, when the competition is increased to 5 (Fig. 4b), red areas start appearing. When the competition increases to 16 (Fig. 4c), the red area is very large and the green area disappears altogether.

In addition, as competition is increased (2 to 5 times), dark orange regions become stronger. These regions are realized when $C_2 + x_2 \geq 10^6$, i.e., the strong population dominates. This results from high competition and low β_2 , allowing the strong population to recover rapidly during extended treatment withdrawal. When the competition reaches 16 times, most of the plot is covered by red regions. This suggests that under high competition, the strong type initially outcompetes the weak type before treatment begins. When a high dose of β_2 is administered, the strong type declines sharply, enabling the weak type to expand significantly. However, with prolonged treatment withdrawal, the strong type can rapidly recover, leading to excessive tumor burden.

To further understand the dynamics of each population in the red area, we perform additional simulations, as

illustrated in Fig. 5. Figure 5 shows the dynamics of the strong and weak types in the red regions. When treatment is administered for an extended period with high β_2 and β_4, the strong type decreases rapidly, allowing the weak type to grow since there is no strong type to suppress its growth.

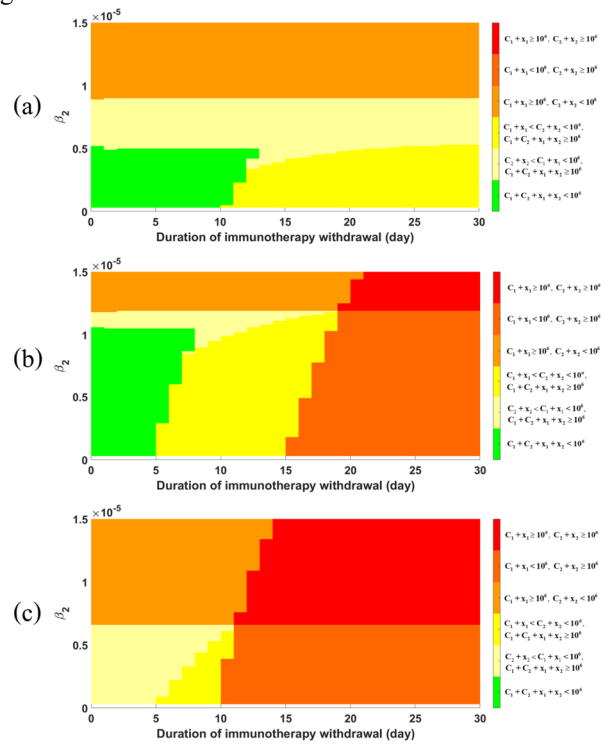

Fig. 4. Simulated total number of cancerous cells with different durations of immunotherapy withdrawal and value of β_2 with fixed treatment duration 30 days, $\beta_4 = 10^{-4}$. (a) competition ratio is two times. (b) competition ratio is five times. (c) competition ratio is sixteen times.

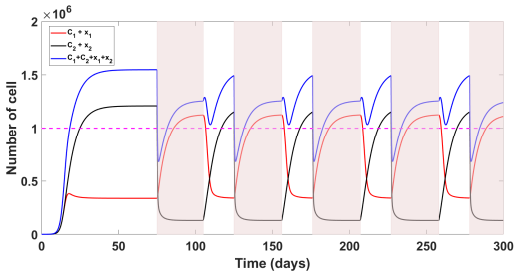

Fig. 5. Population dynamics of cells with competition 16 times, treatment 30 days, and break for 20 days. Fixed $\beta_2 = 10^{-5}$ and $\beta_4 = 10^{-4}$.

However, when treatment is withdrawn for long, the strong type recurs while the weak type declines. This alternating growth pattern between the two types results in the red regions, where both types exceed 10^6, but not simultaneously. Instead, their growth alternates, the strong type grows during treatment withdrawal, while the weak type grows during treatment administration. Overall, these results demonstrate that increasing competition ratios consistently reduce the green area, shifting the parameter space toward regions where the total tumor burden exceeds 10^6. To achieve the optimal outcome, it is essential to carefully balance the dose of β_2 and the duration of immunotherapy withdrawal. These findings emphasize the importance of precise treatment planning to prevent excessive tumor burden.

4 Conclusion

In this study, we investigated the optimal value of β_2 and the immunotherapy withdrawal period. We identified a balance between maintaining $C_2 + x_2$ at levels that are neither too high (dark orange area, dark yellow area) nor too low, as excessively low $C_2 + x_2$ would allow $C_1 + x_1$ to grow uncontrollably (light orange area, light yellow area). When β_4 was fixed at 4×10^{-6} and the treatment duration was varied, we found that longer immunotherapy durations reduced the green area, representing the optimal tumor suppression conditions. This reduction occurs because extended treatment directly suppresses $C_2 + x_2$, leading to a shift from the green area to the light orange area, as $C_1 + x_1$ grows to exceed 10^6. Furthermore, prolonged treatment at high doses of β_2 reduced green area.

In terms of competition ratios, we discovered that higher ratios considerably decreased the green area. As illustrated in Fig. 3, when the competition ratio is two (Fig. 3a), tumor control can be maintained across a relatively broad withdrawal interval of approximately 8 – 10 days for intermediate β_2 values (approximately on the order of 8×10^{-5}). However, when the competition increases to fivefold (Fig. 3b), the admissible withdrawal range narrows to roughly 4 – 6 days under comparable β_2 levels. Under very strong competition (sixteenfold, Fig. 3c), the safe interruption period is further reduced to only about 1 – 3 days. These representative ranges highlight the substantial contraction of the controllable parameter space as intratumoral competition intensifies. Biologically, this contraction may reflect tumors characterized by stronger intratumoral competition, which could be associated with increased cellular heterogeneity or altered microenvironmental interactions. Clinically, this observation suggests that such tumors may have a narrower therapeutic window, requiring more careful dose adjustment and shorter withdrawal intervals to maintain tumor control.

Consequently, higher competition requires increased β_2 dose, while the withdrawal duration should remain short to sustain tumor control. For patients requiring longer treatment durations, a careful balance between the β_2 dose and withdrawal period is essential. In such cases, maintaining a moderate β_2 dose with periodic treatment breaks can provide effective tumor control. Patients in this group have the flexibility to choose between longer or shorter withdrawal intervals as both interventions produce relatively the same effect for inhibiting tumor development. However, extended treatment durations

with high β_2 doses should be prevented as they significantly reduce the green area, indicating the potential for treatment failure.

Overall, these findings define optimal tumor control as a patient-specific approach that considers the complex interplay among intratumoral competition and treatment variables. Optimizing immunotherapy dose and withdrawal timing enables better control the tumor cell population while allowing patients to recover from treatment toxicities.

Although the present model is based on biologically motivated mechanisms, including the enhancement of innate immune activity inspired by nanoparticle-based strategies reported in previous experimental studies [7], the results obtained here are derived from computational simulations. Therefore, further experimental and clinical validation will be required to confirm the applicability of these findings in real therapeutic settings.

This study serves as an important step in the ongoing efforts to design more effective immunotherapy regimens for tumor treatment. The insights gained here contribute to our understanding of the complex dynamics of intratumoral competition and provide a basis for the development of improved treatment strategies.

Acknowledgments

This research project is supported by King Mongkut's University of Technology Thonburi (KMUTT), Thailand Science Research and Innovation (TSRI), and National Science, Research and Innovation Fund (NSRF) Fiscal year 2026. Moreover, this work was also supported by the Science Achievement Scholarship of Thailand.

References

1. S. Ramón y Cajal, M. Sesé, C. Capdevila, T. Aasen, L. De Mattos-Arruda, S. J. Diaz-Cano, J. Hernández-Losa, and J. Castellví, "Clinical implications of intratumor heterogeneity: Challenges and opportunities," *J. Mol. Med.*, vol. 98, no. 2, pp. 161–177, 2020.
2. I. Januskeviciene and V. Petrikaite, "Heterogeneity of breast cancer: The importance of interaction between different tumor cell populations," *Life Sciences*, vol. 239, Art. no. 117009, 2019.
3. M. Raatz, S. Shah, G. Chitadze, M. Brüggemann, and A. Traulsen, "The impact of phenotypic heterogeneity of tumour cells on treatment and relapse dynamics," *PLoS Comput. Biol.*, vol. 17, no. 2, Art. no. e1008702, 2021.
4. Z. Yu, T. G. Pestell, M. P. Lisanti, and R. Pestell, "Cancer stem cells," *Int. J. Biochem. Cell Biol.*, vol. 44, no. 12, pp. 2144–2151, 2012
5. K. Esfahani, L. Roudaia, N. A. Buhlaiga, S. V. Del Rincon, N. Papneja, and W. H. Miller, "A review of cancer immunotherapy: From the past, to the present, to the future," *Current Oncology*, vol. 27, suppl. 2, pp. 87–97, 2020.
6. W. Sukpol, T. Laomettachit, and A. Tangthanawatsakul, "A cancer sub-population competition model reveals optimal levels of immune response that minimize tumor size," *J. Comput. Biol.*, vol. 31, no. 11, pp. 1179–1194, 2023.
7. K. Li, Z. Zhang, Y. Mei, M. Li, Q. Yang, Q. Wu, H. Yang, L. He, and S. Liu, "Targeting the innate immune system with nanoparticles for cancer immunotherapy," *J. Mater. Chem. B*, vol. 10, no. 11, pp. 1709–1733, 2022.
8. A. R. Freischel, M. Damaghi, J. J. Cunningham, A. Ibrahim-Hashim, R. J. Gillies, R. A. Gatenby, and J. S. Brown, "Frequency-dependent interactions determine outcome of competition between two breast cancer cell lines," *Scientific Reports*, vol. 11, no. 1, pp. 1–18, 2021.
9. L. G. De Pillis, A. E. Radunskaya, and C. L. Wiseman, "A validated mathematical model of cell-mediated immune response to tumor growth," *Cancer Research*, vol. 65, no. 17, pp. 7950–7958, 2005.
10. M. Al-Hajj, M. S. Wicha, A. Benito-Hernandez, S. J. Morrison, and M. F. Clarke, "Prospective identification of tumorigenic breast cancer cells," *Proc. Natl. Acad. Sci. U.S.A.*, vol. 100, no. 7, pp. 3983–3988, 2003.
11. L. G. De Pillis, W. Gu, and A. E. Radunskaya, "Mixed immunotherapy and chemotherapy of tumors: Modeling, applications and biological interpretations," *J. Theor. Biol.*, vol. 238, no. 4, pp. 841–862, 2006.
12. C. Enrico Bena, M. Del Giudice, A. Grob, T. Gueudré, M. Miotto, D. Gialama, M. Osella, E. Turco, F. Ceroni, A. De Martino, and C. Bosia, "Initial cell density encodes proliferative potential in cancer cell populations," *Scientific Reports*, vol. 11, no. 1, Art. no. 6101, 2021.
13. I. Kareva and F. Berezovskaya, "Cancer immunoediting: A process driven by metabolic competition as a predator–prey–shared resource type model," *J. Theor. Biol.*, vol. 380, pp. 463–472, 2015.